

## Calcium carbonate precoating/acid cleaning method for fouling control in ceramic nanofiltration membranes

Li, Yuke; Xu, Yidan; Rietveld, Luuk C.; Heijman, Sebastiaan G.J.

**DOI**

[10.1016/j.seppur.2024.130002](https://doi.org/10.1016/j.seppur.2024.130002)

**Publication date**

2024

**Document Version**

Final published version

**Published in**

Separation and Purification Technology

**Citation (APA)**

Li, Y., Xu, Y., Rietveld, L. C., & Heijman, S. G. J. (2024). Calcium carbonate precoating/acid cleaning method for fouling control in ceramic nanofiltration membranes. *Separation and Purification Technology*, 356, Article 130002. <https://doi.org/10.1016/j.seppur.2024.130002>

**Important note**

To cite this publication, please use the final published version (if applicable). Please check the document version above.

**Copyright**

Other than for strictly personal use, it is not permitted to download, forward or distribute the text or part of it, without the consent of the author(s) and/or copyright holder(s), unless the work is under an open content license such as Creative Commons.

**Takedown policy**

Please contact us and provide details if you believe this document breaches copyrights. We will remove access to the work immediately and investigate your claim.



# Calcium carbonate precoating/acid cleaning method for fouling control in ceramic nanofiltration membranes

Yuke Li<sup>\*</sup>, Yidan Xu, Luuk C. Rietveld, Sebastiaan G.J. Heijman

Section of Sanitary Engineering, Department of Water Management, Faculty of Civil Engineering and Geosciences, Delft University of Technology, Stevinweg 1, 2628 CN Delft, the Netherlands

## ARTICLE INFO

Editor: Dr. B. Van der Bruggen

### Keywords:

Ceramic membranes  
Nanofiltration  
CaCO<sub>3</sub> precoat  
Membrane fouling control  
Permeability recovery

## ABSTRACT

Ceramic nanofiltration is a potential one-step treatment for industrial waste streams. It can remove colloidal particles, oil droplets and some organic molecules. The drawback of the technology is that backwash cannot be applied to remove the accumulated cake layer from the membrane surface. At the moment only chemical cleaning with aggressive oxidizing agents like chlorine are effective to restore the permeability of the membranes after fouling. However, calcium carbonate (CaCO<sub>3</sub>) precoating has shown potential benefits in preliminary research, but have only been executed at laboratory scale, under a constant pressure and with a limited number of experimental cycles. In the presented work, the CaCO<sub>3</sub> precoat/acid cleaning method was comprehensively studied under varying operational conditions. Dead-end filtration of a CaCO<sub>3</sub>-dispersion was used to precoat the membrane surface. Three different acids were tested to partly dissolve the precoat and remove the cake layer from the membrane surface. It was found that citric acid performed the best to recover the permeability of the membrane, probably due to the chelating properties, capturing the calcium ions, with a good removal of the cake layer during forward flush as a result. The size of precoat particles influenced the efficacy of permeability recovery. The smaller the deposited precoating particles on the membrane surface were, the better the cleaning effect was. It is expected that, when filtering real sewage water, these membranes can operate with one precoat during about 25 days with five consecutive citric acid cleaning cycles before a chlorine-based chemical treatment should thoroughly clean the membrane module.

## 1. Introduction

Ceramic membrane filtration is an emerging technology for water provision from alternative water sources for e.g. industry [1,2]. A typical ceramic membrane is constructed in an asymmetric multilayered structure consisting of a supporting layer and a thin active separation layer [3]. This multilayer matrix is made of inorganic materials such as zirconia (ZrO<sub>2</sub>), titanium dioxide (TiO<sub>2</sub>), and alumina (Al<sub>2</sub>O<sub>3</sub>), where Al<sub>2</sub>O<sub>3</sub> is mainly used to construct the supporting layer and TiO<sub>2</sub> or ZrO<sub>2</sub> is deposited on the surface of the supporting layer to form a separation layer [4–6]. Compared with polymeric films, the surface functional groups of ceramic layers are single, but rich in metallic hydroxyls, which makes the surface of the layer having a higher hydrophilicity compared

to polymeric membrane surfaces [7,8]. This property is one of the key factors positively influencing organic fouling [9]. Different types of metal oxides have been used to modify the membrane surface to also increase the electrostatic repulsion or the spatial effect between organic pollutants and the membrane [10], so that it can further reduce the adsorption of charged organic pollutants on the membrane and diminish membrane fouling even more [11].

Membrane fouling limits the membrane performance, resulting in a higher transmembrane pressure (TMP), and occasionally, a poor permeate quality. It will further lead to more frequent membrane cleaning, affecting the plant productivity and operational costs [12]. Membrane fouling can be classified into several types based on the nature of the foulants [13]: Particulate fouling, organic & inorganic

*Abbreviations:* ZrO<sub>2</sub>, zirconia; TiO<sub>2</sub>, titanium dioxide; Al<sub>2</sub>O<sub>3</sub>, alumina; TMP, transmembrane pressure; MF, Microfiltration; UF, Ultrafiltration; NF, nanofiltration; PTFE, Polytetrafluoroethylene; CaCO<sub>3</sub>, calcium carbonate; MWCO, molecular weight cut-off; SEM, scanning electron microscopy; EDS, energy dispersive spectroscopy.

<sup>\*</sup> Corresponding author at: Section of Sanitary Engineering, Department of Water Management, Faculty of Civil Engineering and Geosciences, Delft University of Technology, Stevinweg 1, 2628 CN Delft, The Netherlands.

E-mail address: [L.Li-6@tudelft.nl](mailto:L.Li-6@tudelft.nl) (Y. Li).

<https://doi.org/10.1016/j.seppur.2024.130002>

Received 22 July 2024; Received in revised form 21 September 2024; Accepted 3 October 2024

Available online 5 October 2024

1383-5866/© 2024 The Authors. Published by Elsevier B.V. This is an open access article under the CC BY license (<http://creativecommons.org/licenses/by/4.0/>).

fouling, biological fouling and chemical fouling. Wherein, organic and particulate fouling can form a gel-layer, while biodegradable organic matter can result in biological growth [14,15]. At present, advanced technology have been made in reducing membrane fouling in water purification membrane processes, such as tuning membrane hydrophilicity, blending/deposition of inorganic nanomaterials and precoat technology, etc. [16]. For example, Malkapuram [17] found that cellulose acetate (CA)-based nanofiltration membranes prepared with zeolitic imidazolate framework, have been significant improvements in flux and enhanced filtration performance as well as reduced membrane fouling.

A merging strategy for fouling control is precoating the membrane, which has already been applied for both polymeric and ceramic microfiltration (MF) and ultrafiltration (UF), as well as membrane distillation technology [18–21]. A suspension can be applied on membrane surface as precoat, in order to form a permeable and detachable layer. During filtration experiments, the fouling agents accumulate on the precoat layer first and afterwards the membrane is hydraulically backwashed, removing the precoat layer [18,19]. Alternatively, pre-coating using iron or alumina coagulants has been used with the purpose to capture natural organic matter in flocs that can be removed during backwashing of ceramic MF and UF membranes [22]. Also, in terms of membrane distillation precoat fields, Xu [20] found out that, when testing as a protective coating material for PTFE distillation membranes, those pre-coated with glycerol addition performed higher thermal stability, mechanical strength and lower water sorption capacity than those without precoat.

However, during ceramic nanofiltration (NF) backwashing cannot be performed to remove the precoat and cake layer, because, apart from a limited backwash velocity compared to MF and UF, the membrane can be damaged due to high pressures on the permeate site [23], mainly at the seals of the ceramic NF membrane. Thus, chemical cleaning is the most common method applied for ceramic NF [24,25]. As an alternative a calcium carbonate ( $\text{CaCO}_3$ ) precoat with acid dosing during forward flush has been studied with positive results [23]. However, the previous

study was executed under constant pressure with small, single channel membranes, while experiments with larger membranes under constant flux conditions are more representative for full-scale plant applications. Therefore, in this work, the  $\text{CaCO}_3$  precoat/acid cleaning method was comprehensively studied with variation in coating particle size, coating amount and mechanisms in different acids for cleaning.

## 2. Materials and methods

### 2.1. Membranes characteristics

Commercially available ceramic NF membranes, which were produced by Inopor GmbH, Germany, were used with a support layer of  $\alpha\text{-Al}_2\text{O}_3$  and an active layer of titanium oxide ( $\text{TiO}_2$ ). The modules were monolithic ceramic NF membranes with 19 channels of 3.5 mm diameter in each channel and length of 0.5 m and specific membrane area of  $0.1045 \text{ m}^2$ . The used ceramic NF membranes had 450 Da as a nominal molecular weight cut-off (MWCO), with open porosity of 30–40 %, and an average pore size of 0.9 nm, as indicated by the supplier [23]. Caltran and Shang, et al. [26,27], determined the factual MWCO of the membrane, by measuring the retention of polyethylene glycol (PEG, provided by Sigma-Aldrich, Germany) with 5 molecular weights (200, 300, 400, 600, 1000, Da) as solution tracers. High performance size exclusion chromatography (Prominence, Shimadzu, Japan), which was fortified with a gel permeation column (5 mm  $30 \text{ \AA}$ , PSS GmbH, Germany) and a deflective index indicator (RID-20A, Shimadzu, Japan), was used for PEG samples analyzation [28].

### 2.2. $\text{CaCO}_3$ nano-particle preparation-zeta potential

To explore how different sizes of  $\text{CaCO}_3$  influence the effectiveness of fouling control, small sized  $\text{CaCO}_3$  particles were prepared by mixing calcium chloride and sodium bicarbonate. Different larger  $\text{CaCO}_3$  particles were purchased from Sigma-Aldrich and Riedel-de Haën. To realize a decent distribution of  $\text{CaCO}_3$  particles in solution and avoid

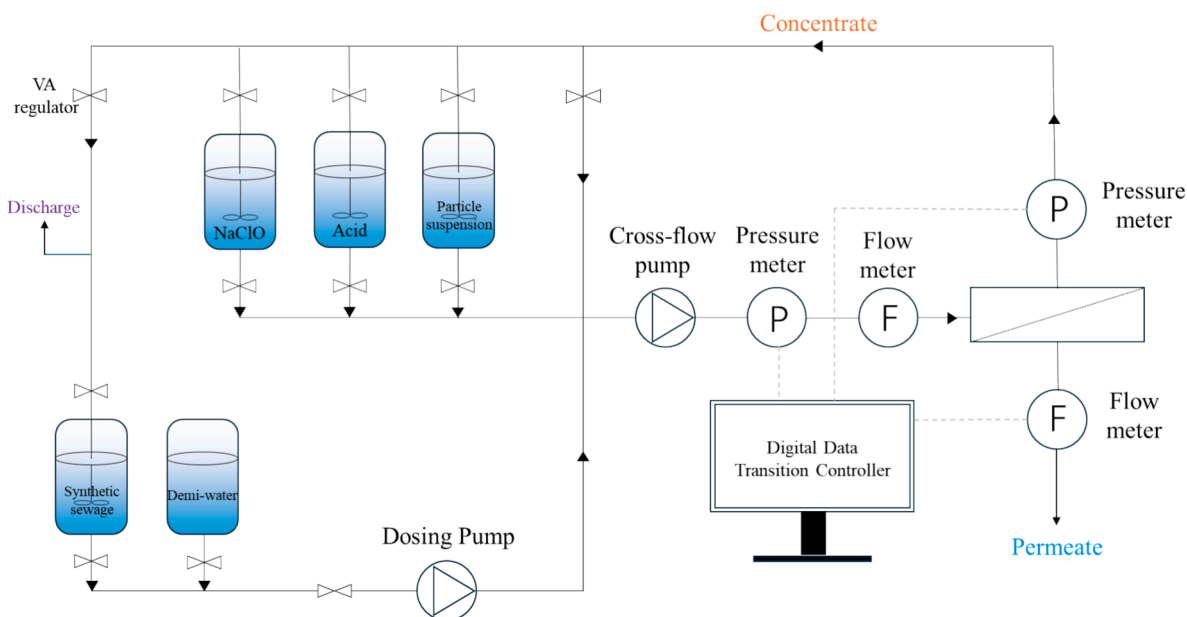


Fig. 1. Diagram for cross-flow ceramic NF bench scale installation.

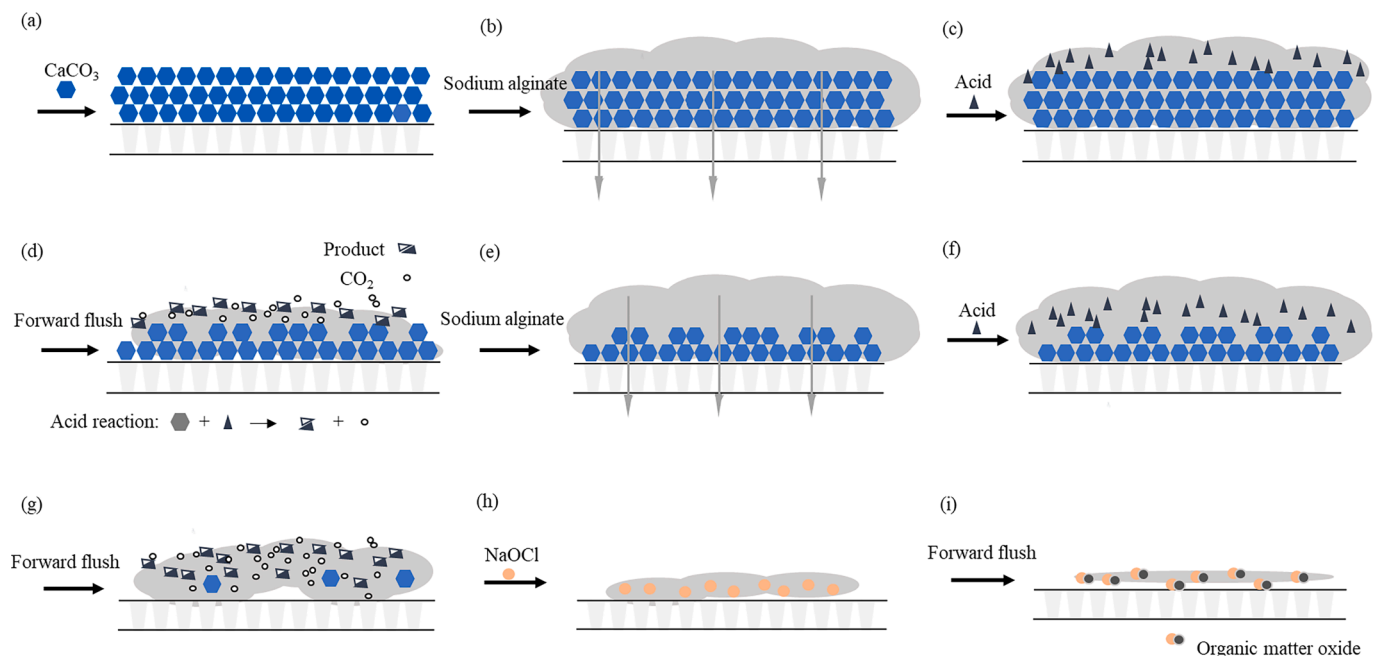


Fig. 2. Schematic diagram of the reaction precoating method using the  $\text{CaCO}_3$  particles.

aggregation on the long run, the stability of the dispersion was increased by increasing the zeta potential of the dispersion. To increase the zeta potential and the surface charge of the nanosized  $\text{CaCO}_3$  an excess of calcium ( $\text{Ca}^{2+}$ ) ions in the solution was applied [29]. Therefore, the concentration of the  $\text{Ca}^{2+}$  ions was varied from 0 to 9 mM, and the concentration of  $\text{HCO}_3^-$  ions from 0 to 11.75 mM. The zeta potential value was then measured by ZETASIZER (Mavern). All coating solutions were dispersed in a solution with the same concentration of  $\text{Ca}^{2+}$  and  $\text{HCO}_3^-$ .

### 2.3. Model sewage

Sodium alginate was selected as a typical gel-like contaminant to form a gel deposited layer on the surface of the membranes [30], and it is commonly used as model compound in membrane fouling experiments [31]. The model sewage solution was composed of 0.4 g·L<sup>-1</sup> sodium alginate, 1 mM  $\text{NaHCO}_3$  as buffer, 5 mM  $\text{NaCl}$  as background salt concentration, and 3 mM  $\text{CaCl}_2$  to adjust the pH in the range of 7.0 to 7.5. Above chemicals were supplied by Sigma-Aldrich company.  $\text{Ca}^{2+}$  was added, because it preferentially binds with the carboxyl groups of the sodium alginate, thus bridging the adjacent molecules, forming the so-called “egg-box” model fouling [31]. Kramer’s research [25] showed that after 5 days of real wastewater filtration experiments, the permeability reduced 58 % and the ceramic nanofiltration membrane had a serious membrane fouling issue. By using high concentration model sewage, fouling of the membrane is enhanced and substantial fouling could be obtained in 40 min filtration time, representing approximately five days of operation under normal conditions in raw sewage water.

### 2.4. Filtration set-up

The experiments were executed at constant flux with a feed pump to pressurize the system and a cross-flow pump to provide a constant cross-

flow velocity. Five feed water solutions were used during the fouling/cleaning cycles: (i) demineralized water for initial permeability tests and for the forward flush after acid cleaning, (ii) a  $\text{CaCO}_3$  dispersion for precoating, (iii) model sewage (sodium alginate solution) for fouling, (iv) different types of acid for acid cleaning, and (v) sodium hypochlorite for ultimate chemical cleaning after each experiment. All feed waters, except the demineralized water feedwater, was recirculated to a feed vessel (Fig. 1).

The permeate flux was kept constant at 20 l·m<sup>-2</sup>·h<sup>-1</sup> (35 ml·min<sup>-1</sup>), the cross-flow velocity was kept at 0.67 m·s<sup>-1</sup>, aiming to obtain turbulent condition into the tubular membrane [32], and the TMP varied during the experiment from 1 to 10 bar.

To determine the permeability during fouling tests, due to slight changes in environmental temperature, the following, temperature corrected [33], permeability was used (see equation (1) [34]).

$$L_{20^\circ\text{C}} = \frac{J \cdot e^{-0.0239 \cdot (T-20)}}{\Delta P} \quad (1)$$

where:

- $L$ : the temperature corrected permeability in l·(m<sup>2</sup>·h·bar)<sup>-1</sup>;
- $T$ : the temperature of water (°C);
- $J$ : the membrane flux (l·m<sup>-2</sup>·h<sup>-1</sup>);
- $\Delta P$ : the TMP (bar).

Membrane permeability recovery illustrated the effectiveness of membrane cleaning method and Eq. (2) was used to determine the recovery.

$$\text{Permeability Recovery} = \frac{L_{i,0} - L_{1,e}}{L_{1,0} - L_{1,e}} \quad (2)$$

where:

- $L_{1,0}$ : initial permeability in cycle I, l·(m<sup>2</sup>·h·bar)<sup>-1</sup>;
- $L_{1,e}$ : final permeability in cycle I, l·(m<sup>2</sup>·h·bar)<sup>-1</sup>;
- $L_{i,0}$ : initial permeability in cycle i, l·(m<sup>2</sup>·h·bar)<sup>-1</sup>;

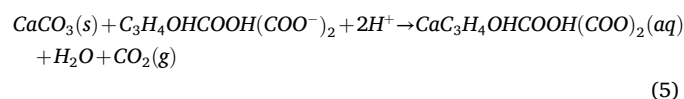
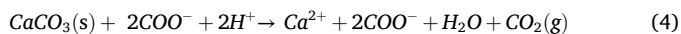
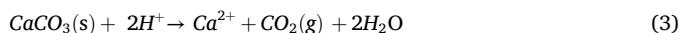
$L_{i,e}$ : final permeability in cycle  $i$ ,  $l \cdot (\text{m}^2 \cdot \text{h} \cdot \text{bar})^{-1}$ .

In terms of comparing the changes in permeability recovery, permeability Normalization needs to be calculated by  $L_i/L_0$ , where  $L_0$  is the initial permeance of the filtration experiment. The temperature was measured together with the two pressures (in the feed and the concentrate of the ceramic membrane and in the permeate flow). In this way the variation of the permeability in time was obtained. The initial permeability was measured before the fouling tests started, being referred to as the clean membrane permeability. In addition, the permeability was measured after fouling and cleaning, using demineralized water as well, to quantify the effect of the cleaning on fouling removal. The initial permeability was also tested after the  $\text{CaCO}_3$  precoat, to explore the membrane permeability loss due to the coating layer.

## 2.5. Application of the $\text{CaCO}_3$ precoat and acid cleaning

Cross-sectional views of the  $\text{CaCO}_3$ -coated membranes were observed by scanning electron microscopy (SEM, Hitachi S-3400 II, Japan), which is installed with energy dispersive spectroscopy (EDS) [35]. The precoat solution was filtrated on the membrane surface under dead-end conditions, with pressures from 8 to 10 bar (fluxes of 90 to  $110 \text{ l} \cdot \text{m}^{-2} \cdot \text{h}^{-1}$ ). It ensured that  $\text{CaCO}_3$  is deposited to the surface of the membrane.

After fouling, three different acids were used for acid cleaning: Hydrochloric acid, formic acid, and citric acid. The reactions of the acid with the  $\text{CaCO}_3$  coating are shown in Equations (3), (4) and (5).



After the acid reaction with the precoat, forward flushing was executed (with demineralized water) for removing the reaction products and cake layer from the membrane surface. After 10 min of forward flush under low pressures, another fouling cycle was carried out. The cycle of fouling and acid cleaning was operated three or six times without replacing/renewing the precoat. Fig. 2 illustrates the probable mechanisms of the acid reaction-based method with  $\text{CaCO}_3$  coat, by steps. Firstly,  $\text{CaCO}_3$  as precoat was pressed on the membrane surface. Then model sewage water (sodium alginate solution) was filtrated through the membrane as fouling process. After fouling, acid was added to react with the precoat and generated acid reaction products and carbon dioxide. Finally, the fouling layer was removed by a forward flush. When the precoat was consumed, sodium hypochlorite was used to remove the residual foulant on the surface and inside the pores of membrane and demineralized water was flushed in forward direction to recover the ceramic NF membrane entirely. All filtration experiments were duplicated with 5 % error [36], to confirm the reproducibility and feasibility [37].

## 2.6. Chlorine cleaning

After each experiment with multiple fouling and acid cleaning cycles, the membrane set-up was thoroughly cleaned, to remove all fouling

and precoat and to start the next experiment with a clean membrane. Sodium hypochlorite was used as effective chemical cleaning agent [38], the used concentration was 0.2 % for rinsing during 30 min. In case of residual  $\text{CaCO}_3$  on the membrane surface, HCl (0.01 mol/l) [39] was used for rinsing the membranes for 5 min.

## 3. Results and discussion

### 3.1. Influence of $\text{CaCO}_3$ particle size on the cleaning efficiency

The  $\text{CaCO}_3$  particles were suspended and well-dispersed in a solution with  $\text{Ca}^{2+}$  and  $\text{HCO}_3^-$  [29,40]. The charge of the particles, measured as zeta potential, was manipulated by changing the  $\text{Ca}^{2+}$  ions' and bicarbonate  $\text{HCO}_3^-$  ions' concentrations in the  $\text{CaCO}_3$  dispersion [29,41], while the pH of the solution was kept at 7.5. The zeta potential of the  $\text{CaCO}_3$  solution without  $\text{CaCl}_2$  and  $\text{NaHCO}_3$  was 9.8 mV. Because the dispersion was not stable at this low zeta potential this led to particle agglomeration and sedimentation. Whereas, when dosing 9 mM  $\text{Ca}^{2+}$  and 7.5 mM  $\text{HCO}_3^-$ , the zeta potential was +25.9 mV (Table 1), and even after 24 h the particles remained dispersed as the particle size distribution shows (Fig. 3). A higher  $\text{HCO}_3^-$  concentration caused a decline in the zeta potential, while a higher  $\text{Ca}^{2+}$  concentration resulted in an increase in zeta potential. The three different particle sizes of  $\text{CaCO}_3$  were measured by a particle size analyzer (PSD). The smallest  $\text{CaCO}_3$  average size of particles were  $0.13 \mu\text{m}$  (Fig. 3.(a)). The average size of  $\text{CaCO}_3$  particles from Riedel-de Haën were  $1.7 \mu\text{m}$  (Fig. 3.(c)), whereas the  $\text{CaCO}_3$  particles average size from Sigma-Aldrich were  $10.5 \mu\text{m}$  (Fig. 3.(e)). All coating solutions were dispersed in a solution with the same concentration of  $\text{Ca}^{2+}$  and  $\text{HCO}_3^-$ . Due to the larger spaces between particles, the fouling cake layer is likely to directly adhere the membrane surface, forming irreversible fouling [42], which resulted in a decrease in permeance, as shown in the Fig. 3(b),(d) & Fig. 4.

The effectiveness of the various  $\text{CaCO}_3$  particle sizes was studied after 120 min of fouling. The precoat of  $\text{CaCO}_3$  was combined with a citric acid cleaning, when using the  $0.13 \mu\text{m}$   $\text{CaCO}_3$  dispersion as a precoat, the permeability recovery was the largest with 93 % after the first cycle and 68 % recovery after the second cycle, respectively (see Fig. 4 & Table 2). The reason that the smaller particles performed better than the larger particles was probably due to effective filtration by the coating, avoiding the foulants to reach the membrane through the particle layer, which can also be the reason for the limited fouling in the first cycle. With the smallest particle size, thus, a cake layer was formed on top of the precoat, which could also be more effectively removed during the acid reaction and flushing, compared to the precoat with the other particle sizes.

**Table 1**  
zeta potential of  $\text{CaCO}_3$  solutions.

| $\text{CaCO}_3$<br>(g/l) | $\text{CaCl}_2$<br>(mM) | $\text{NaHCO}_3$<br>(mM) | Zeta potential<br>(mV) |
|--------------------------|-------------------------|--------------------------|------------------------|
| 0.4                      | 0                       | 0                        | 9.78                   |
| 0.4                      | 3                       | 7.5                      | 17.6                   |
| 0.4                      | 6                       | 7.5                      | 21.4                   |
| 0.4                      | 9                       | 7.5                      | 25.9                   |
| 0.4                      | 9                       | 9                        | 23.8                   |

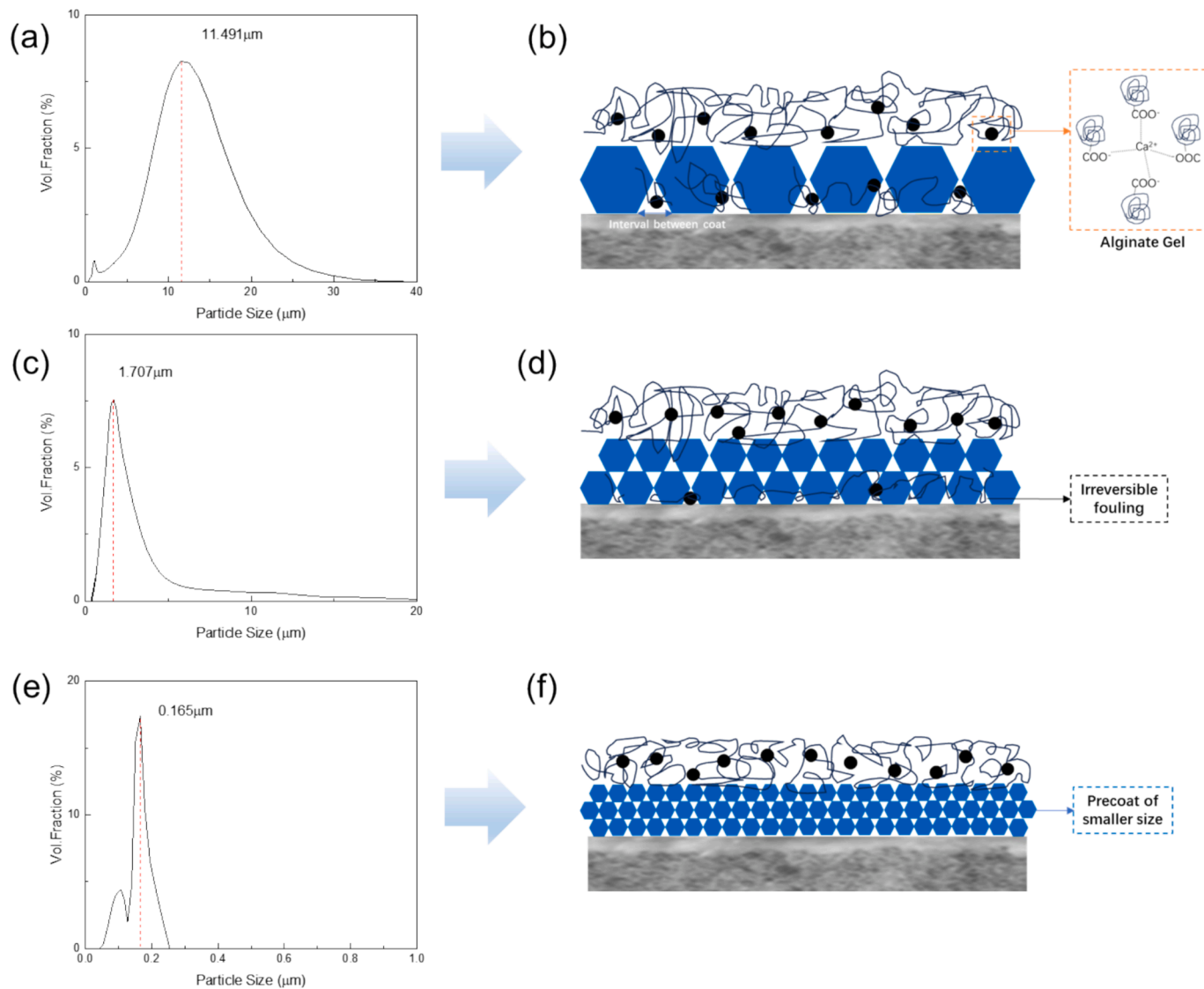


Fig. 3. (a),(c),(e) Three different precoat particle size; (b),(d),(f) Mechanism diagram of particle size influence towards membrane fouling.

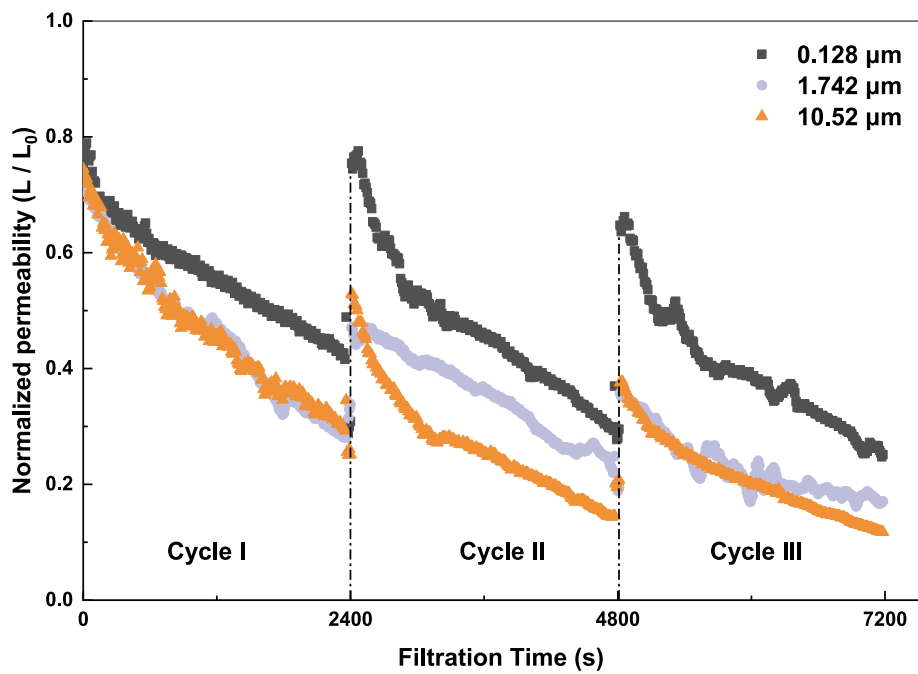


Fig. 4. Comparison of different coating sizes on the precoated membrane.

**Table 2**  
Permeability recovery with different coating particle size.

| Acid cleaning   | 0.13 $\mu\text{m}$ permeability recovery | 1.742 $\mu\text{m}$ permeability recovery | 10.52 $\mu\text{m}$ permeability recovery |
|-----------------|--|---|---|
| First cleaning  | 93 %                                     | 57 %                                      | 50 %                                      |
| Second cleaning | 68 %                                     | 23 %                                      | 17 %                                      |

### 3.2. Characterization of $\text{CaCO}_3$ pre-coated membranes

A 0.4 g/l  $\text{CaCO}_3$  dispersion of 0.13  $\mu\text{m}$  was deposited on the membrane by dead-end filtration, with a permeate flux  $110 \text{ l}\cdot\text{m}^{-2}\cdot\text{h}^{-1}$  for 7 min under 9 bars of TMP, to ensure sufficient attachment on the membrane surface. Because the particles sizes were larger than the pore size of the NF membrane ( $<1 \text{ nm}$ ), the  $\text{CaCO}_3$  particles were deposited on the membrane surface without entering the membrane pores (Fig. 5.(a)). Fig. 5.(b) showed the crystal structure shape of precoat is spherical and ellipsoidal [43]. The thickness of the coating layer was estimated from the pictures in Fig. 5.(b), being on average 8.09  $\mu\text{m}$ . The  $\text{CaCO}_3$  coating was much thicker than that of  $\text{TiO}_2$  active membrane layers (50 nm, specifications of the producer), potentially acting as a pre-filtration media for the sodium alginate solution before fouling the active NF-membrane layer [44]. The actual MWCO was measured by the rejection rate of PEG of different sizes, and the specific curve was shown in the Fig. 5(c). The actual measured MWCO is different from the 450 Da

data provided by the Inopor GmbH company, which has been verified in other similar membrane studies [27,28,45,46].

### 3.3. Restoration of permeability with and without coating

The initial permeability, measured using demineralized water, was in the average of  $14\text{--}20 \text{ l}\cdot(\text{m}^2\cdot\text{h}\cdot\text{bar})^{-1}$  with a constant permeate flux of  $20 \text{ l}\cdot\text{m}^{-2}\cdot\text{h}^{-1}$  and a cross-flow velocity of  $0.67 \text{ m}\cdot\text{s}^{-1}$ . Citric acid, formic acid and hydrochloric acid were tested during the cleaning process. The pH of the hydrochloric acid (10 mM) was 2.0, while the formic (10 mM) and citric acid (10 mM) solutions had a pH 2.62 and 2.91, respectively. Cleaning the pristine membrane with citric acid achieved a permeability recovery of 14 %, while with formic acid it had a 21 % permeability increase, and with HCl cleaning a permeability increase of 34 % was observed (see Fig. 6.). These results confirm earlier studies where it was found that organic fouling is removed by either a base (such as NaOH) or an oxidizing chemical (such as Chlorine) [47] rather than an acid.

The results further show that citric acid cleaning performed the best regarding permeability recovery of the pre-coated membrane. An abrupt decline of the permeability took place at the start of the fouling experiment, probably due to alginate adsorption [48]. Fig. 7. shows that cleaning the coated membrane with citric acid resulted in an 86 % permeability increase after the first cycle and a 74 % increase after the second cycle. Formic acid cleaning performed slightly less with an 76 % permeability increase after the first cycle and a 63 % increase after the second cycle, while HCl cleaning resulted in only 75 % and 45 % permeability recovery after the first and second cycle, respectively

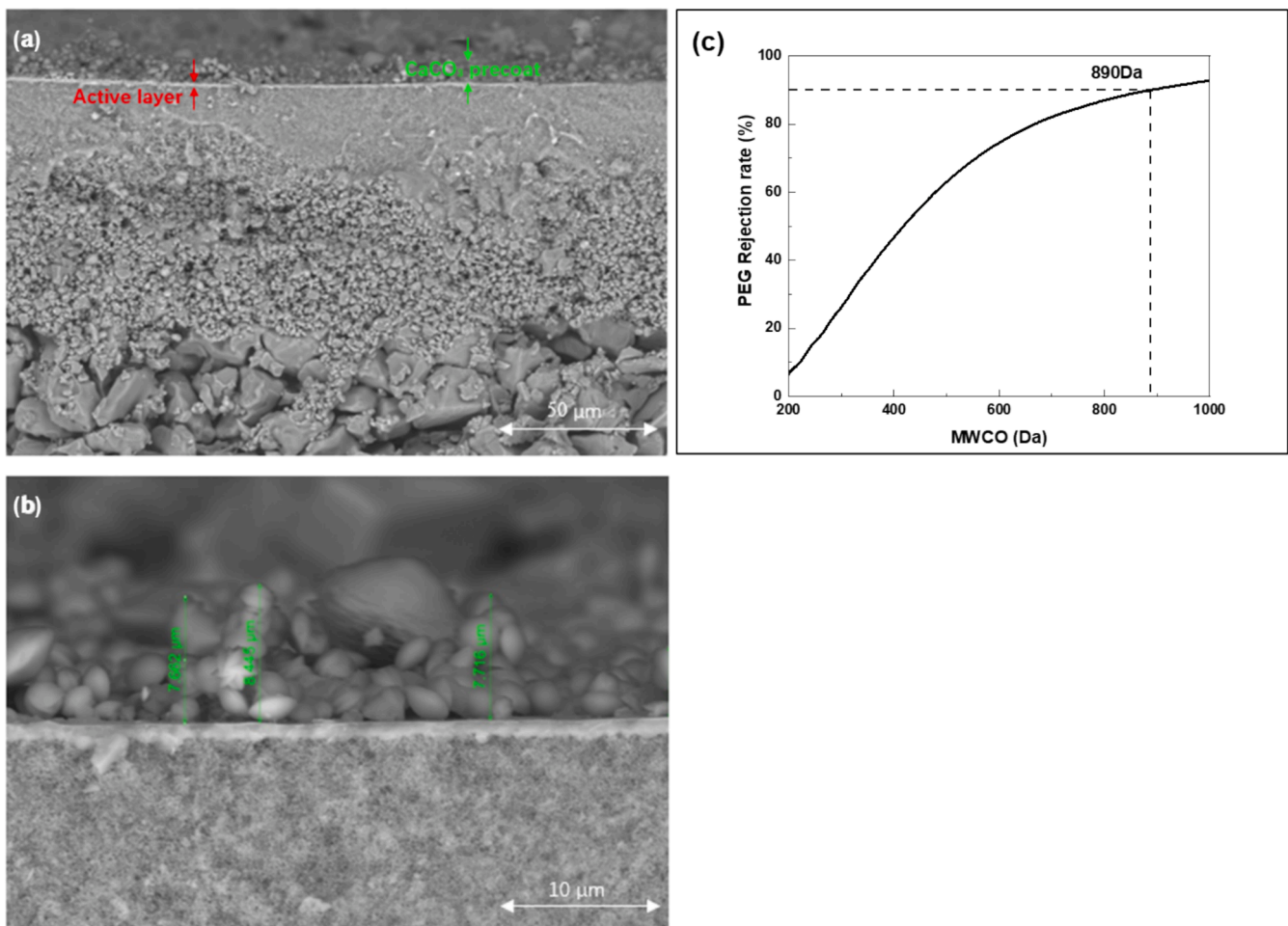


**Fig. 5.** Characterization of precoat ceramic NF membranes: (a) cross-section SEM image of  $\text{CaCO}_3$  pre-coated membrane; (b) and thickness of the  $\text{CaCO}_3$  layer; (c) Polyethylene glycol (PEG) retention rate curve of NF.

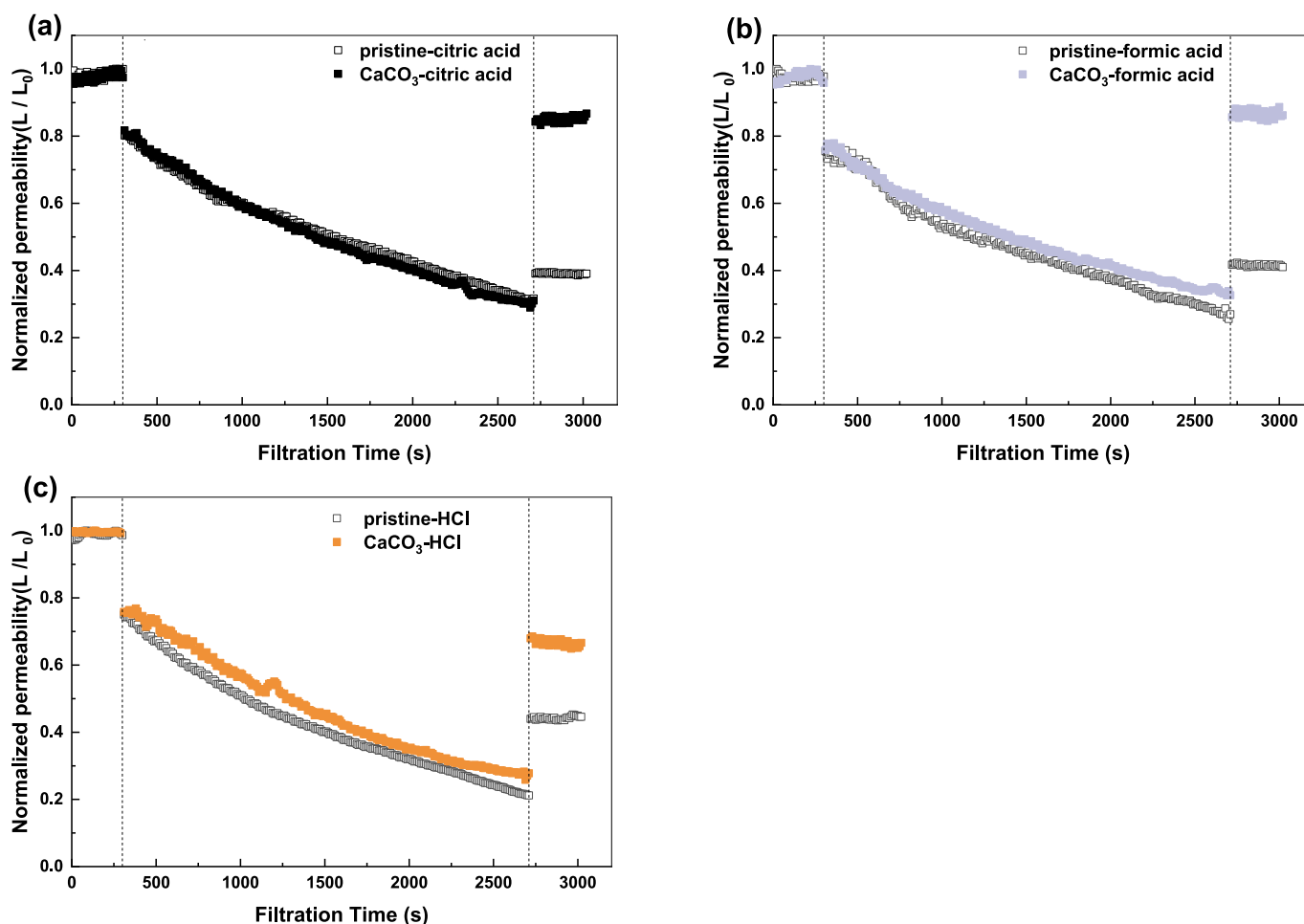


Fig. 6. Normalized permeability of both the pristine membranes and  $\text{CaCO}_3$  pre-coated membranes after (a) citric acid cleaning; (b) formic acid cleaning; (c) and hydrochloric acid cleaning.

(Table 3). In addition, after HCl cleaning the permeability decline due to fouling was more pronounced compared to the fouling curve after formic and citric acid cleaning. Citric acid is a chelating agent [49], containing three carboxyl groups ( $-\text{COOH}$ ) and formic acid is a monocarboxylic acid, having affinity towards  $\text{Ca}^{2+}$  ions to produce complex substances (Fig. 8), which could assist in the loosening and detachment of the  $\text{CaCO}_3$  – sodium alginate layer [50–52]. Besides, the chelates with a larger molecular weight could provide sufficient adsorption sites for sodium alginate, stimulating the flushing of sodium alginate and contributing to a higher permeability recovery after citric acid cleaning. However, in the case of HCl, no complexes or chelates were produced to help the detachment of most sodium alginate. Therefore, the recovery of  $\text{CaCO}_3$  – HCl acid cleaning was probably lowest, and residual foulants were still attached on surface of the membrane. In addition, in the case of HCl cleaning, the fouling was accelerated compared to formic and citric acid cleaning, probably because the  $\text{CaCO}_3$  was dissolved unevenly so some parts of the membrane coating were completely removed, and the membrane surface was thus fully exposed to the foulant in the subsequent cycle.

The consumption of the coating after acid cleaning was also measured (Fig. 7.b). It was confirmed that HCl dissolved the highest amount of  $\text{CaCO}_3$  precoat after three cycles, which was 338 mg (188 mg after the first cycle and 150 mg the after second cycle), about 56 % of the coating, while formic acid dissolved 300 mg of the  $\text{CaCO}_3$  precoat (188 mg after the first cycle and 113 after the second cycle), and citric acid consumed only 238 mg of  $\text{CaCO}_3$  precoat (125 mg after the first cycle and the 113 after second cycle). Lower pH of HCl and formic acid caused

the pre-coating to overreact with the acid and lack of buffering [53]. In this case, the pre-coating consumption amount was larger, but the cleaning effect was not as remarkable as that of citric acid with higher pH.

#### 3.4. Multiple cycle tests with precoat fouling tests and citric acid cleaning

As shown in Fig. 9, at a pre-coating amount of ( $5742 \text{ mg/m}^2$ ) 600 mg of  $\text{CaCO}_3$ , the initial permeability was only 3 % lower than that without a pre-coating. As the calcium carbonate coating increases, the initial permeability begins to decline in a gradient. This is mainly due to the increased thickness of the pre-coated layer and the high resistance [28,42]. It resulted in an 18 % decrease in the initial permeability of ( $9570 \text{ mg/m}^2$ ) 1000 mg of  $\text{CaCO}_3$  pre-coating. Therefore, it is necessary to use ( $7655 \text{ mg/m}^2$ ) 800 mg of  $\text{CaCO}_3$  (the permeability decreased by 9 %, which is still within a reasonable range) as a multi-layer pre-coating for multi-cycle filtration experiments. To test the performance of cleaning with citric acid on the pre-coated membranes for longer-term usage, experiments were conducted during six cycles (of 40 min each) with  $7655 \text{ mg/m}^2$  (800 mg)  $\text{CaCO}_3$ , using a coating particle size of  $0.13 \mu\text{m}$  deposited on the membranes, a constant flux of  $20 \text{ l}\cdot\text{m}^{-2}\cdot\text{h}^{-1}$  and a cross-flow velocity of  $0.67 \text{ m}\cdot\text{s}^{-1}$  (see Fig. 9&10). Since one cycle corresponds to 5 days in filtration of untreated domestic sewage with 58 % of permeability reduction [25], Fig. 10.(a) indicated that the average permeability dropped by 60 % per cycle. In comparison, the results suggested that about 25 days of operation could be expected without a chlorine-based chemical cleaning. Frequent chemical cleaning can lead



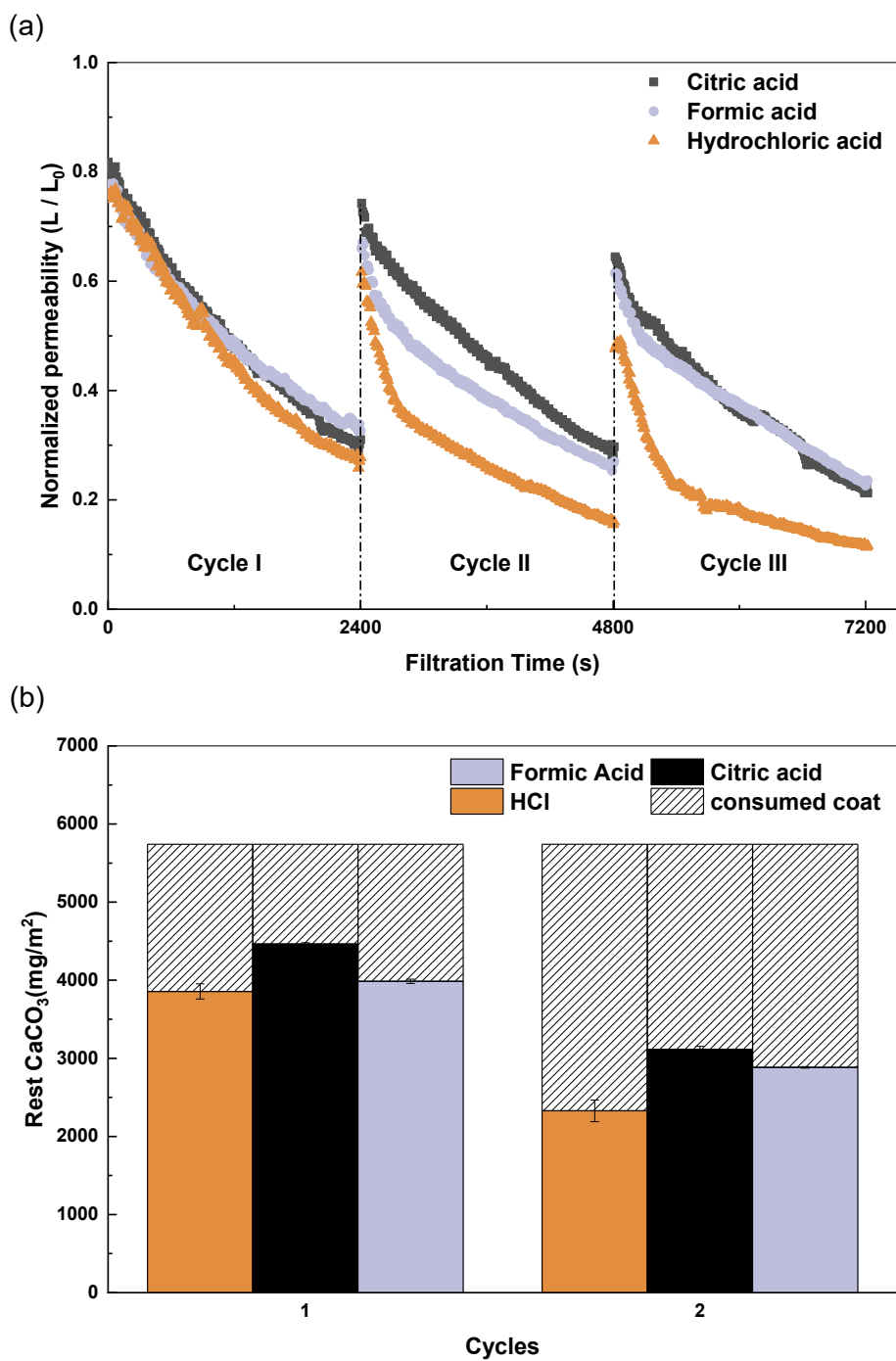


Fig. 7. (a) Comparison of citric acid, formic acid and hydrochloric acid on the pre-coated membrane (b) CaCO<sub>3</sub> consumption after different acids reactions.

**Table 3**  
Permeability recovery after three acid cleaning methods.

| Acid cleaning   | Citric acid permeability recovery | Formic acid permeability recovery | Hydrochloric acid permeability recovery |
|-----------------|-----------------------------------|-----------------------------------|---|
| First cleaning  | 86 %                              | 76 %                              | 70 %                                    |
| Second cleaning | 67 %                              | 63 %                              | 45 %                                    |

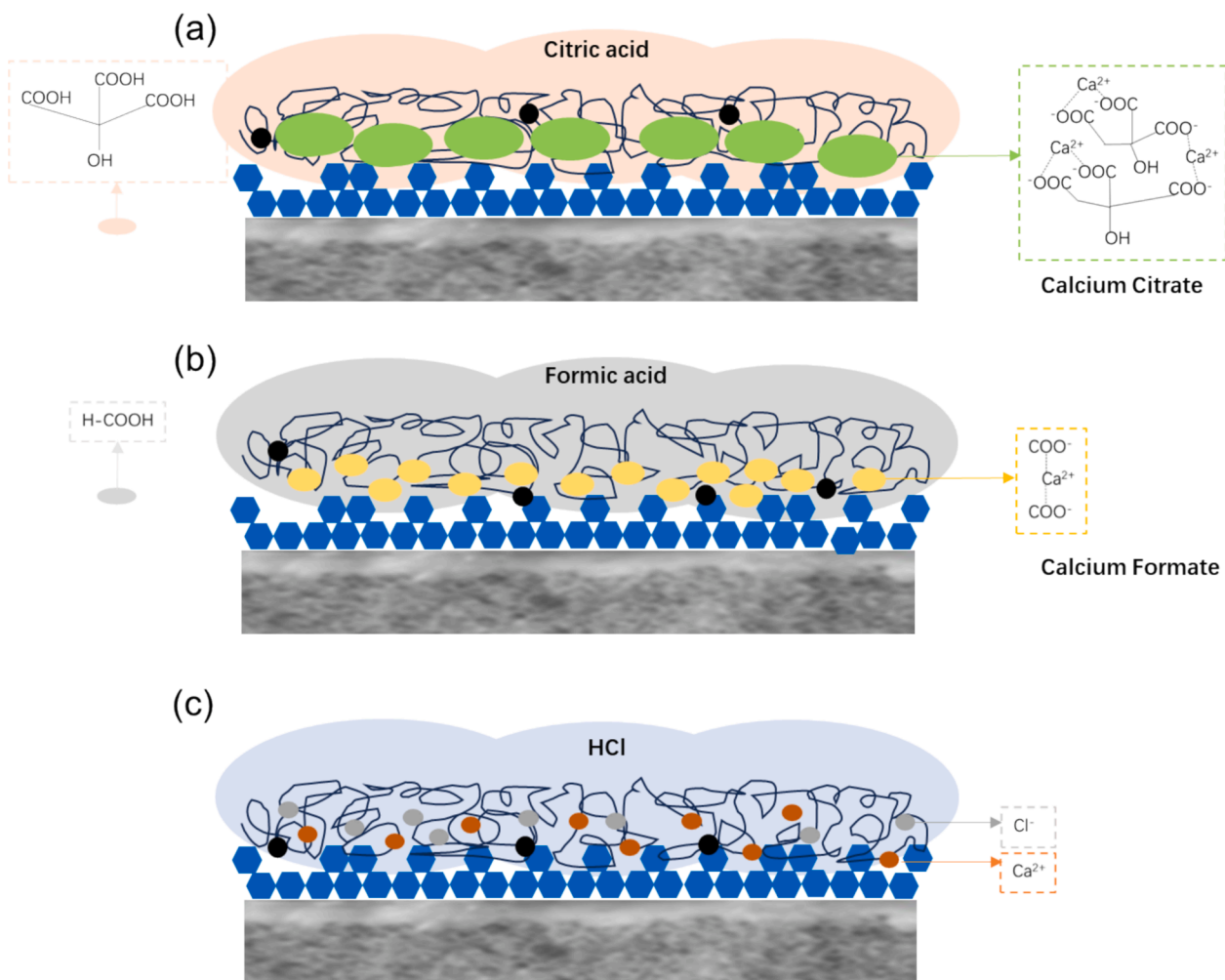


Fig. 8. Mechanism diagram of (a) citric acid (b)Formic acid (c) HCl acid cleaning effect towards membrane fouling removal.

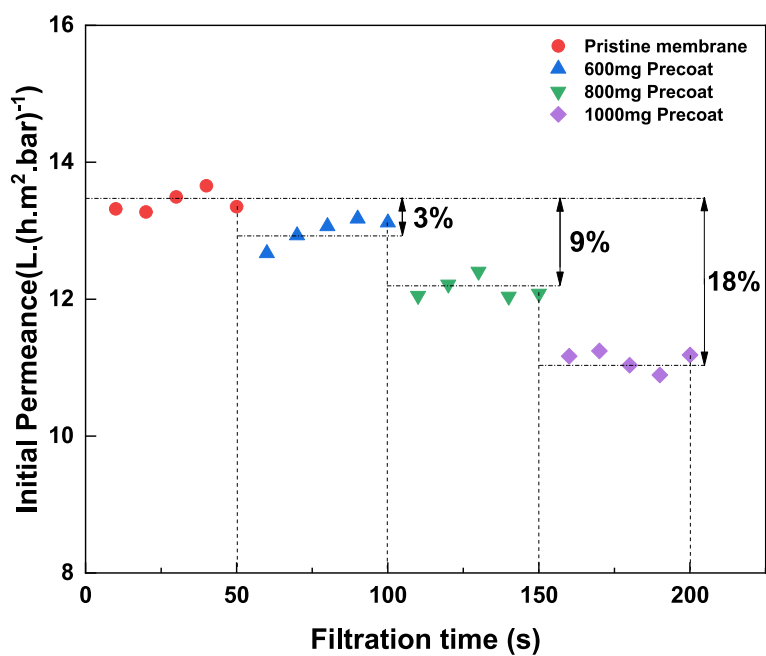


Fig. 9. Comparison of initial permeance without pre-coating and with different amounts of pre-coating in fouling filtration experiments.

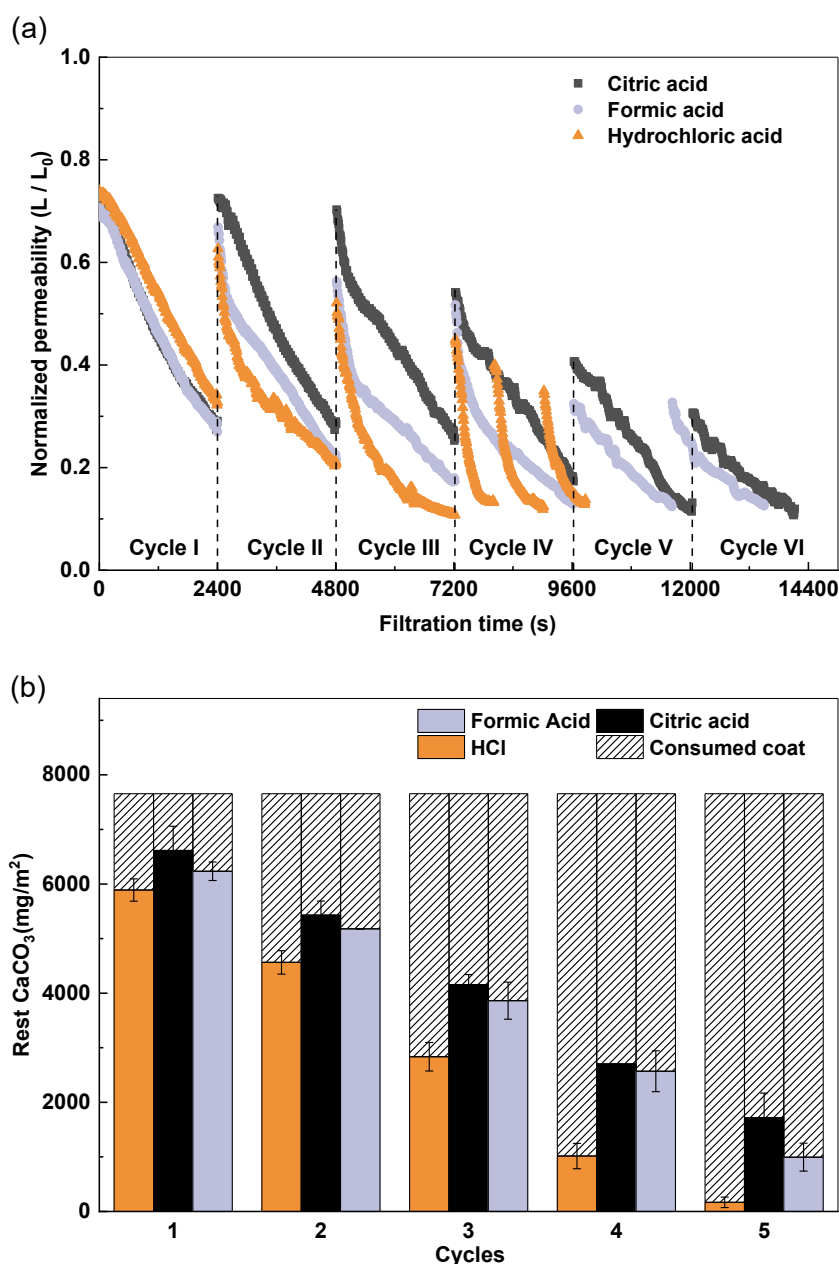


Fig. 10. (a) Six cycles of fouling tests under cleaning with citric acid on the precoated membrane (b)  $\text{CaCO}_3$  consumption after citric acid reactions.

**Table 4**  
Permeability recovery after acids cleaning methods for 6 cycles.

| Acid cleaning   | Citric acid permeability recovery | Formic acid permeability recovery | Hydrochloric acid permeability recovery |
|-----------------|-----------------------------------|-----------------------------------|---|
| First cleaning  | 95 %                              | 82 %                              | 76 %                                    |
| Second cleaning | 88 %                              | 68 %                              | 48 %                                    |
| Third cleaning  | 58 %                              | 57 %                              | 31 %                                    |
| Fourth cleaning | 30 %                              | 13 %                              | 19 %                                    |
| Fifth cleaning  | 9 %                               | 12 %                              | 6 %                                     |

to membrane degradation and shorter membrane lifespan [54]. The application of  $\text{CaCO}_3$  precoat in combination with citric acid cleaning could thus greatly reduce the frequency of chemical cleaning (Table 4), thereby extending the life of the ceramic NF membrane and diminishing the impact on the environment [55]. From Fig. 10(a), it can be observed that from the fourth cycle onwards, the membrane cleaned with HCl, and formic acid cleaning fouled too quickly and could not complete the filtration test (40 min) anymore.

#### 4. Conclusion and perspective

$\text{CaCO}_3$  precoating combined with acid cleaning was studied for cleaning sodium alginate gel-like fouling of ceramic NF membranes. The conclusions are summarized in the following aspects:

- Coating solutions remained well dispersed with a zeta potential of + 25.9 mV.

- The smaller precoat  $\text{CaCO}_3$  particles protected the membrane against fouling better than the larger  $\text{CaCO}_3$  particles and were thus more effective as a precoat.
- Citric acid cleaning performed best with the highest permeability recovery of the  $\text{CaCO}_3$  precoat membrane, with 86 % after first cycle and 67 % after second cycle. The complexing (chelating) of calcium ions with the citric acid carboxylic groups, in combination with adsorption of sodium alginate, probably enhances the cleaning process.
- Six fouling-acid cleaning cycles with 40 min filtration time, a flux of  $20 \text{ l}\cdot\text{m}^{-2}\cdot\text{h}^{-1}$  and a cross-flow velocity of  $0.67 \text{ m}\cdot\text{s}^{-1}$  were effective with a starting precoat of  $7655 \text{ mg CaCO}_3/\text{m}^2$ . Meanwhile, the initial permeance with precoat was only reduced by 9 %.
- It is expected that, when filtering real sewage water, these membranes can operate with one precoat during about 25 days with five consecutive citric acid cleaning cycles before a chlorine-based chemical treatment should thoroughly clean the membrane module.
- Applying domestic or industrial sewage as influent to further verify the feasibility of the  $\text{CaCO}_3$  precoat method in practice. Because of much slower fouling of raw sewage water, pilot experiments are needed with acid/cleaning cycles about every 5 days.

### CRediT authorship contribution statement

**Yuke Li:** Conceptualization, Methodology, Investigation, Writing – original draft. **Yidan Xu:** Writing – original draft. **Luuk C. Rietveld:** Writing – review & editing, Supervision. **Sebastiaan G.J. Heijman:** Conceptualization, Methodology, Writing – review & editing, Supervision.

### Declaration of competing interest

The authors declare that they have no known competing financial interests or personal relationships that could have appeared to influence the work reported in this paper.

### Data availability

Data will be made available on request.

### Acknowledgement

The authors acknowledge the PhD scholarship awarded to Yuke Li (No. 201907720010) by the China Scholarship Council, China.

### References

- [1] Y. Dong, H. Wu, F. Yang, S. Gray, Cost and efficiency perspectives of ceramic membranes for water treatment, *Water Res.* 220 (2022) 118629, <https://doi.org/10.1016/j.watres.2022.118629>.
- [2] A. Loi-Brügger, S. Panglisch, P. Buchta, K. Hattori, H. Yonekawa, Y. Tomita, R. Gimbel, Ceramic membranes for direct river water treatment applying coagulation and microfiltration, *Water Sci. Technol. Water Supply* 6 (4) (2006) 89–98, <https://doi.org/10.2166/ws.2006.906>.
- [3] E. Drioli, L. Giorno, *Comprehensive membrane science and engineering*. Vol. 1. (2010): Newnes. 282–296 Doi: 10.1016/B978-0-12-409547-2.12221-8.
- [4] J. Kim, B. Van der Bruggen, The use of nanoparticles in polymeric and ceramic membrane structures: review of manufacturing procedures and performance improvement for water treatment, *Environ. Pollut.* 158 (7) (2010) 2335–2349, <https://doi.org/10.1016/j.envpol.2010.03.024>.
- [5] S. Anisah, M. Kanezashi, H. Nagasawa, T. Tsuru, Hydrothermal stability and permeation properties of  $\text{TiO}_2\text{-ZrO}_2$  (5/5) nanofiltration membranes at high temperatures, *Sep. Purif. Technol.* 212 (2019) 1001–1012, <https://doi.org/10.1016/j.seppur.2018.12.006>.
- [6] M. Al-Shaeli, O.O. Teber, R.A. Al-Juboori, A. Khataee, I. Koyuncu, V. Vatanpour, Inorganic layered polymeric membranes: Highly-ordered porous ceramics for surface engineering of polymeric membranes, *Sep. Purif. Technol.* (2024), <https://doi.org/10.1016/j.seppur.2024.127925>, 127925.
- [7] S.-J. Lee, J.-H. Kim, Differential natural organic matter fouling of ceramic versus polymeric ultrafiltration membranes, *Water Res.* 48 (2014) 43–51, <https://doi.org/10.1016/j.watres.2013.08.038>.
- [8] S.-J. Lee, M. Dilaver, P.-K. Park, J.-H. Kim, Comparative analysis of fouling characteristics of ceramic and polymeric microfiltration membranes using filtration models, *J. Membr. Sci.* 432 (2013) 97–105, <https://doi.org/10.1016/j.memsci.2013.01.013>.
- [9] F. Xiao, P. Xiao, W. Zhang, D. Wang, Identification of key factors affecting the organic fouling on low-pressure ultrafiltration membranes, *J. Membr. Sci.* 447 (2013) 144–152, <https://doi.org/10.1016/j.memsci.2013.07.040>.
- [10] D. Lu, T. Zhang, L. Gutierrez, J. Ma, J.-P. Croué, Influence of surface properties of filtration-layer metal oxide on ceramic membrane fouling during ultrafiltration of oil/water emulsion, *Environ. Sci. Tech.* 50 (9) (2016) 4668–4674, <https://doi.org/10.1021/acs.est.5b04151>.
- [11] S. Byun, S. Davies, A. Alpatova, L. Corneal, M. Baumann, V. Tarabara, S. Masten, Mn oxide coated catalytic membranes for a hybrid ozonation–membrane filtration: comparison of Ti, Fe and Mn oxide coated membranes for water quality, *Water Res.* 45 (1) (2011) 163–170, <https://doi.org/10.1016/j.watres.2010.08.031>.
- [12] P.H. Wolf, S. Siversns, S. Monti, UF membranes for RO desalination pretreatment, *Desalination* 182 (1–3) (2005) 293–300, <https://doi.org/10.1016/j.desal.2005.05.006>.
- [13] Charcosset, *Comprehensive Biotechnology*. Comprehensive Biotechnology, (2011) <http://doi.org/10.1016/B978-0-08-088504-9.00131-8>.
- [14] S.G.S. Rodriguez, Particulate and Organic Matter Fouling of Seawater Reverse Osmosis Systems: Characterization, Modelling and Applications. UNESCO-IHE PhD Thesis. (2011): CRC Press Doi: 10.1201/b11609.
- [15] T. Nguyen, F.A. Roddick, L. Fan, Biofouling of water treatment membranes: a review of the underlying causes, monitoring techniques and control measures, *Membranes* 2 (4) (2012) 804–840, <https://doi.org/10.3390/membranes2040804>.
- [16] R. Castro-Muñoz, A critical review on electrospun membranes containing 2D materials for seawater desalination, *Desalination* 555 (2023) 116528, <https://doi.org/10.1016/j.desal.2023.116528>.
- [17] S.T. Malkapuram, M.M. Seepana, S.H. Sonawane, S.K. Lakhera, E. Randviir, ZIF-8 decorated cellulose acetate mixed matrix membrane: An efficient approach for textile effluent treatment, *Chemosphere* 349 (2024) 140836, <https://doi.org/10.1016/j.carbpol.2022.120230>.
- [18] G. Galjaard, P. Buijs, E. Beerendonk, F. Schoonenberg, J.C. Schippers, Pre-coating (EPCE®) UF membranes for direct treatment of surface water, *Desalination* 139 (1–3) (2001) 305–316, [https://doi.org/10.1016/S0011-9164\(01\)00324-1](https://doi.org/10.1016/S0011-9164(01)00324-1).
- [19] G. Galjaard, J. Kruihof, H. Scheerman, J. Verdouw, J. Schippers, Enhanced pre-coat engineering (EPCE®) for micro-and ultrafiltration: steps to full-scale application, *Water Sci. Technol. Water Supply* 3 (5–6) (2003) 125–132, <https://doi.org/10.2166/ws.2003.0158>.
- [20] J. Xu, D. Spittler, J. Bartley, R. Johnson, Alginate acid–silica hydrogel coatings for the protection of osmotic distillation membranes against wet-out by surface-active agents, *J. Membr. Sci.* 260 (1–2) (2005) 19–25, <https://doi.org/10.1016/j.memsci.2005.03.017>.
- [21] A. Ali, M.M.A. Shirazi, L. Nthunya, R. Castro-Muñoz, N. Ismail, N. Tavajohi, G. Zaragoza, C.A. Quist-Jensen, Progress in module design for membrane distillation, *Desalination* 581 (2024) 117584, <https://doi.org/10.1016/j.desal.2024.117584>.
- [22] H. Yonekawa, Y. Tomita, Y. Watanabe, Behavior of micro-particles in monolith ceramic membrane filtration with pre-coagulation, *Water Sci. Technol.* 50 (12) (2004) 317–325, <https://doi.org/10.2166/wst.2004.0729>.
- [23] F. Kramer, R. Shang, L. Rietveld, S. Heijman, Fouling control in ceramic nanofiltration membranes during municipal sewage treatment, *Sep. Purif. Technol.* 237 (2020) 116373, <https://doi.org/10.1016/j.seppur.2019.116373>.
- [24] M. Zebić Avdičević, K. Košutić, S. Dobrović, Effect of operating conditions on the performances of multichannel ceramic UF membranes for textile mercerization wastewater treatment, *Environ. Technol.* 38 (1) (2017) 65–77, <https://doi.org/10.1080/09593330.2016.1186225>.
- [25] F.C. Kramer, R. Shang, S.G. Heijman, S.M. Scherrenberg, J.B. van Lier, L. C. Rietveld, Direct water reclamation from sewage using ceramic tight ultra-and nanofiltration, *Sep. Purif. Technol.* 147 (2015) 329–336, <https://doi.org/10.1016/j.seppur.2015.04.008>.
- [26] R. Shang, A. Goulas, C.Y. Tang, X. de Frias Serra, L.C. Rietveld, S.G. Heijman, Atmospheric pressure atomic layer deposition for tight ceramic nanofiltration membranes: Synthesis and application in water purification, *J. Membr. Sci.* 528 (2017) 163–170, <https://doi.org/10.1016/j.memsci.2017.01.023>.
- [27] I. Caltran, L. Rietveld, H. Shorney-Darby, S. Heijman, Separating NOM from salts in ion exchange brine with ceramic nanofiltration, *Water Res.* 179 (2020) 115894, <https://doi.org/10.1016/j.watres.2020.115894>.
- [28] B. Lin, S.G. Heijman, L.C. Rietveld, Catalytic pre-coat on ceramic nanofiltration membranes for segregation and Fenton cleaning of high-resistance colloids in direct surface water treatment, *J. Membr. Sci.* 694 (2024) 122401, <https://doi.org/10.1016/j.memsci.2023.122401>.
- [29] P. Moulin, H. Roques, Zeta potential measurement of calcium carbonate, *J. Colloid Interface Sci.* 261 (1) (2003) 115–126, [https://doi.org/10.1016/S0021-9797\(03\)00057-2](https://doi.org/10.1016/S0021-9797(03)00057-2).
- [30] P. van den Brink, A. Zwijnenburg, G. Smith, H. Temmink, M. van Loosdrecht, Effect of free calcium concentration and ionic strength on alginate fouling in cross-flow membrane filtration, *J. Membr. Sci.* 345 (1–2) (2009) 207–216, <https://doi.org/10.1016/j.memsci.2009.08.046>.
- [31] K. Katsoufidou, S.G. Yiantsios, A.J. Karabelas, Experimental study of ultrafiltration membrane fouling by sodium alginate and flux recovery by backwashing, *J. Membr. Sci.* 300 (1–2) (2007) 137–146, <https://doi.org/10.1016/j.memsci.2007.05.017>.

- [32] P.J. LaNasa, E.L. Upp. Fluid flow measurement: A practical guide to accurate flow measurement. (2014): Butterworth-Heinemann Doi: 10.1016/B978-0-12-409524-3.00002-2.
- [33] X. Du, Y. Shi, V. Jegatheesan, I.U. Haq, A review on the mechanism, impacts and control methods of membrane fouling in MBR system, *Membranes* 10 (2) (2020) 24, <https://doi.org/10.3390/membranes10020024>.
- [34] M. Mulder, *Basic principles of membrane technology*. (1996): Springer science & business media. 280-415 Doi: 10.1007/978-94-009-1766-8.
- [35] C. Gabrielli, R. Jaouhari, S. Joiret, G. Maurin, P. Rousseau, Study of the electrochemical deposition of CaCO<sub>3</sub> by in situ Raman spectroscopy: I. Influence of the substrate, *J. Electrochem. Soc.* 150 (7) (2003) C478, <https://doi.org/10.1149/1.1579482>.
- [36] A. Imbrogno, M.N. Nguyen, A.I. Schäfer, Tutorial review of error evaluation in experimental water research at the example of membrane filtration, *Chemosphere* (2024) 141833, <https://doi.org/10.1016/j.chemosphere.2024.141833>.
- [37] P.B. Stark, Before reproducibility must come preproducibility, *Nature* 557 (7706) (2018) 613–614, <https://doi.org/10.1038/d41586-018-05256-0>.
- [38] S. Fukuzaki, Mechanisms of actions of sodium hypochlorite in cleaning and disinfection processes, *Biocontrol Sci.* 11 (4) (2006) 147–157, <https://doi.org/10.4265/bio.11.147>.
- [39] I.B. Ivanishin, H.A. Nasr-El-Din, Effect of calcium content on the dissolution rate of dolomites in HCl acid, *J. Pet. Sci. Eng.* 202 (2021) 108463, <https://doi.org/10.1016/j.petrol.2021.108463>.
- [40] Q. Shi, S. Zhang, G.P. Korfiatis, C. Christodoulatos, X. Meng, Identifying the existence and molecular structure of the dissolved HCO<sub>3</sub>-Ca-As (V) complex in water, *Sci. Total Environ.* 724 (2020) 138216, <https://doi.org/10.1016/j.scitotenv.2020.138216>.
- [41] Y.C. Huang, F.M. Fowkes, T.B. Lloyd, N.D. Sanders, Adsorption of calcium ions from calcium chloride solutions onto calcium carbonate particles, *Langmuir* 7 (8) (1991) 1742–1748, <https://doi.org/10.1021/la00056a028>.
- [42] C. Tzotzi, T. Pahiadaki, S. Yiantsios, A. Karabelas, N. Andritsos, A study of CaCO<sub>3</sub> scale formation and inhibition in RO and NF membrane processes, *J. Membr. Sci.* 296 (1–2) (2007) 171–184, <https://doi.org/10.1016/j.memsci.2007.03.031>.
- [43] H.-Q. Jin, H. Athreya, S. Wang, K. Nawaz, Experimental study of crystallization fouling by calcium carbonate: Effects of surface structure and material, *Desalination* 532 (2022) 115754, <https://doi.org/10.1016/j.desal.2022.115754>.
- [44] B. Lin, S.G.J. Heijman, R. Shang, L.C. Rietveld, Integration of oxalic acid chelation and Fenton process for synergistic relaxation-oxidation of persistent gel-like fouling of ceramic nanofiltration membranes, *J. Membr. Sci.* 636 (2021), <https://doi.org/10.1016/j.memsci.2021.119553>.
- [45] Y. So, Y. Lee, S. Kim, J. Lee, C. Park, Role of co-existing ions in the removal of dissolved silica by ceramic nanofiltration membrane, *J. Water Process Eng.* 53 (2023) 103873, <https://doi.org/10.1016/j.jwpe.2023.103873>.
- [46] G. Mustafa, K. Wyns, A. Buekenhoudt, V. Meynen, Antifouling grafting of ceramic membranes validated in a variety of challenging wastewaters, *Water Res.* 104 (2016) 242–253, <https://doi.org/10.1016/j.watres.2016.07.057>.
- [47] L.D. Nghiem, T. Fujioka, Removal of emerging contaminants for water reuse by membrane technology, *Emerg. Membr. Technol. Sustain. Water Treatm.* (2016) 217–247, <https://doi.org/10.1016/B978-0-444-63312-5.00009-7>.
- [48] B. Lin, L.C. Rietveld, L. Yao, S.G. Heijman, Adsorption and cake layer fouling in relation to Fenton cleaning of ceramic nanofiltration membranes, *J. Membr. Sci.* (2023) 122097, <https://doi.org/10.1016/j.memsci.2023.122097>.
- [49] X. Li, B. Gao, Q. Yue, D. Ma, H. Rong, P. Zhao, P. Teng, Effect of six kinds of scale inhibitors on calcium carbonate precipitation in high salinity wastewater at high temperatures, *J. Environ. Sci.* 29 (2015) 124–130, <https://doi.org/10.1016/j.jes.2014.09.027>.
- [50] M. Ghoorah, B.Z. Dlugogorski, R.D. Balucan, E.M. Kennedy, Selection of acid for weak acid processing of wollastonite for mineralisation of CO<sub>2</sub>, *Fuel* 122 (2014) 277–286, <https://doi.org/10.1016/j.fuel.2014.01.015>.
- [51] A. Karar, F. Naamoune, A. Kahoul, Chemical and electrochemical study of the inhibition of calcium carbonate precipitation using citric acid and sodium citrate, *Desalin. Water Treat.* 57 (35) (2016) 16300–16309, <https://doi.org/10.1080/19443994.2015.1077743>.
- [52] A.I. Mitsionis, T.C. Vaimakis, C.C. Trapalis, The effect of citric acid on the sintering of calcium phosphate bioceramics, *Ceram. Int.* 36 (2) (2010) 623–634, <https://doi.org/10.1016/j.ceramint.2009.09.034>.
- [53] J.L. Haan, R.I. Masel, The influence of solution pH on rates of an electrocatalytic reaction: Formic acid electrooxidation on platinum and palladium, *Electrochim. Acta* 54 (16) (2009) 4073–4078, <https://doi.org/10.1016/j.electacta.2009.02.045>.
- [54] V. Gitis, R.C. Haught, R.M. Clark, J. Gun, O. Lev, Application of nanoscale probes for the evaluation of the integrity of ultrafiltration membranes, *J. Membr. Sci.* 276 (1–2) (2006) 185–192, <https://doi.org/10.1016/j.memsci.2005.09.055>.
- [55] S.H. Park, Y.G. Park, J.-L. Lim, S. Kim, Evaluation of ceramic membrane applications for water treatment plants with a life cycle cost analysis, *Desalin. Water Treat.* 54 (4–5) (2015) 973–979, <https://doi.org/10.1080/19443994.2014.912162>.